Multipolar interference effects in nanophotonics

Wei Liu[1] and Yuri S. Kivshar[2,3]

[1]College of Optoelectronic Science and Engineering, National University of Defense Technology, Changsha, Hunan 410073, People's Republic of China
[2]Nonlinear Physics Centre, Research School of Physics and Engineering, Australian National University, Canberra, Australian Capital Territory 2601, Australia
[3]Department of Nanophotonics and Metamaterials, ITMO University, St Petersburg 197101, Russia

WL, 0000-0002-7067-6239; YSK, 0000-0002-3410-812X

Scattering of electromagnetic waves by an arbitrary nanoscale object can be characterized by a multipole decomposition of the electromagnetic field that allows one to describe the scattering intensity and radiation pattern through interferences of dominating multipole modes excited. In modern nanophotonics, both generation and interference of multipole modes start to play an indispensable role, and they enable nanoscale manipulation of light with many related applications. Here, we review the multipolar interference effects in metallic, metal–dielectric and dielectric nanostructures, and suggest a comprehensive view on many phenomena involving the interferences of electric, magnetic and toroidal multipoles, which drive a number of recently discussed effects in nanophotonics such as unidirectional scattering, effective optical antiferromagnetism, generalized Kerker scattering with controlled angular patterns, generalized Brewster angle, and non-radiating optical anapoles. We further discuss other types of possible multipolar interference effects not yet exploited in the literature and envisage the prospect of achieving more flexible and advanced nanoscale control of light relying on the concepts of multipolar interference through full phase and amplitude engineering.

This article is part of the themed issue 'New horizons for nanophotonics'.
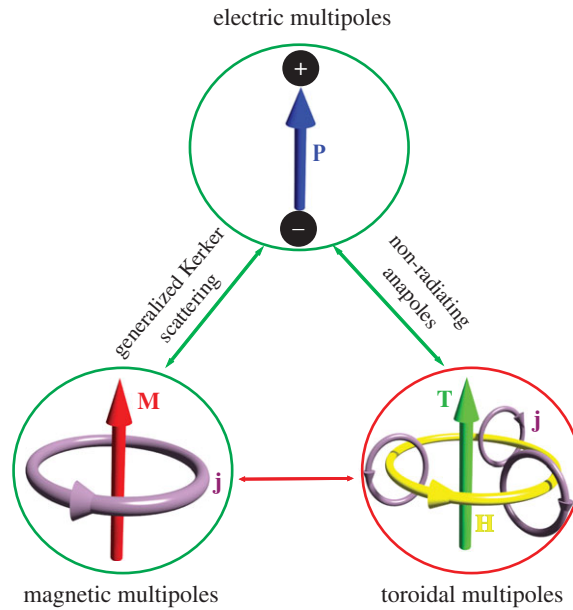
Figure 1. Schematic of interference effects discussed in this review. We consider interferences for three families of electromagnetic multipoles: electric, magnetic and toroidal multipoles. The circles denote interferences between multipoles from the same family, while the double arrows stand for interferences between multipoles from different families. The corresponding charge–current distributions for the dipoles of each family are shown within the circles (**P**, ED moment; **M**, MD moment; **T**, TD moment; **j**, electric current; **H**, magnetic field). The green (red) colour denotes the effects that have (have not) been studied in the existing literature in the field of nanophotonics. (Online version in colour.)

1. Introduction

Stimulated by new concepts in the physics of metamaterials and metasurfaces and the rapid development of nanoscale fabrication technologies, the field of nanophotonics has experienced an explosive growth in recent years, which enables various applications relying on flexible and efficient subwavelength light manipulations (e.g. [1–14]). Similar to conventional photonics operating at other spatial scales, the fundamental research and applications in nanophotonics rely significantly on resonant light–matter interactions, where the detailed analysis of the excitation and interference of electromagnetic multipoles are usually crucial and indispensable [7,8,15–17]. Conventional multipole expansions have mostly been conducted for dynamic charge–current distributions on length scales that are much smaller than the effective wavelength of light, where consequently only the electric and magnetic dipoles are dominant [15,17,18]. Nevertheless, when the dynamic charge–current is distributed within an area comparable to or larger than the effective wavelength of light, higher order multipoles including dynamic toroidal multipoles will arise, and they would contribute to generate electromagnetic fields [15,17–19]. To characterize accurately the photonic features and to optimize a design of nanostructures for achieving desired functionalities, comprehensive investigations should be conducted into the physics of interference between all three families of dynamic electromagnetic multipoles, which may open an extra dimension for nanoscale light manipulation and incubate more in-depth fundamental research and realistic applications in nanophotonics.

In this review, for the first time to our knowledge, we present a brief while coherent view on different types of interference effects that may occur for the three families of classical dynamic multipole radiation modes, namely *electric, magnetic and toroidal multipoles*. We discuss how such interferences enable various recently predicted or observed novel effects with nanoscale structures guiding the manipulation of light and related functionalities at the nanoscale. The

corresponding charge–current distributions for the lowest order dipoles, such as electric dipole (ED), magnetic dipole (MD) and toroidal dipole (TD), are shown schematically in figure 1. The interference effects we discuss here can roughly be divided into two categories: (i) interferences between multipoles from the same family (circles) and (ii) interferences between multipoles from different families (double arrows). In §§2 and 3, we review, respectively, the interferences between electric multipoles and those between magnetic multipoles. The interferences between electric and magnetic multipoles are discussed in §4, where we focus mainly on the generalized Kerker scattering and other induced effects such as the generalized Brewster angle and broadband high-efficient light control with metasurfaces. In §5, we summarize the recent studies of interference effects involving electric and toroidal multipoles, also highlighting the concept of *non-radiating anapoles* realized with simple individual nanoparticles. Other types of possible interferences include the interferences between toroidal multipoles and interferences between magnetic and toroidal multipoles, as presented by the red double arrow and red circle in figure 1, and are discussed briefly in §6 that concludes the paper.

2. Electric multipoles

In the field of nanophotonics, the investigations into interference between electric multipoles are most comprehensive, as magnetic and toroidal multipoles have attracted attention only since the emergence of the field of metamaterials [7,8,17,19]. Before that, it had been long taken for granted that most nanostructures show dominantly electric responses with negligible magnetic responses, especially in the optical regime. As a result, there has been a significant amount of studies focusing on the electric responses only, where the analysis on the excitation and interferences of EDs plays a fundamental role [1,4,6,9,14]. Radiation of an individual ED is symmetric, distributing energy equally into the two opposite directions perpendicular to the dipole orientation (figure 2a). Some combinations of several EDs with engineered phases and amplitudes can render more freedom for radiation pattern shaping, which is highly desired for many applications in nanophotonics, such as sensing, nanoantennas and photovoltaic devices [1–3,6,11]. A well-known example to break the radiation symmetry is the Yagi–Uda antenna [6], where reflectors and directors are employed to route the radiation of the driven dipole to a preferred direction. In figure 2a, we show a much simpler while widely employed configuration of two coupled EDs with $\pi/2$ phase difference and $\lambda/4$ displacement. A simple phase analysis reveals that the radiated fields of the two EDs interfere constructively and destructively towards the right and left, respectively, leading to a highly asymmetric scattering pattern compared with that of an individual ED (figure 2a) [20]. This is exactly the mechanism of the so-called anti-reflection coatings in optics [15,16].

A generalized version of the ED pair is that with the phase difference and displacement properly tuned, then the constructive scattering enhancement can be observed at other radiation angles. An example of this is shown in figure 2b, where a pair of silver and gold discs can be viewed as two coupled EDs, and they can route light of different colours into different preferred directions [21]. This occurs due to the fact that for different wavelengths the phase accumulated through the optical path and the intrinsic phase difference (induced by different complex polarizabilities for two different material-dependent plasmon resonances [16]) between two EDs of the metallic discs vary, resulting in the functionality of flexible colour routing. A more recent exploitation of the concept of ED pairs is shown in figure 2c, where it is demonstrated that incident circularly polarized light of different handedness can be coupled to surface plasmon polariton (SPP) modes propagating in two opposite directions [22]. The mechanism of such a helicity-dependent propagation is exactly the same as that shown in figure 2a, while here the circular polarization of incident waves provides two perpendicular metal-bar EDs in each unit cell with an absolute $\pi/2$ phase difference. A different handedness can be employed to flip the sign of the phase difference and thus change the direction of SPP waves. Alternatively, such a helicity-dependent phase can be interpreted as a Pancharatnam–Berry phase [25–27], based on which many other more sophisticated nanophotonics structures can be designed to enable more
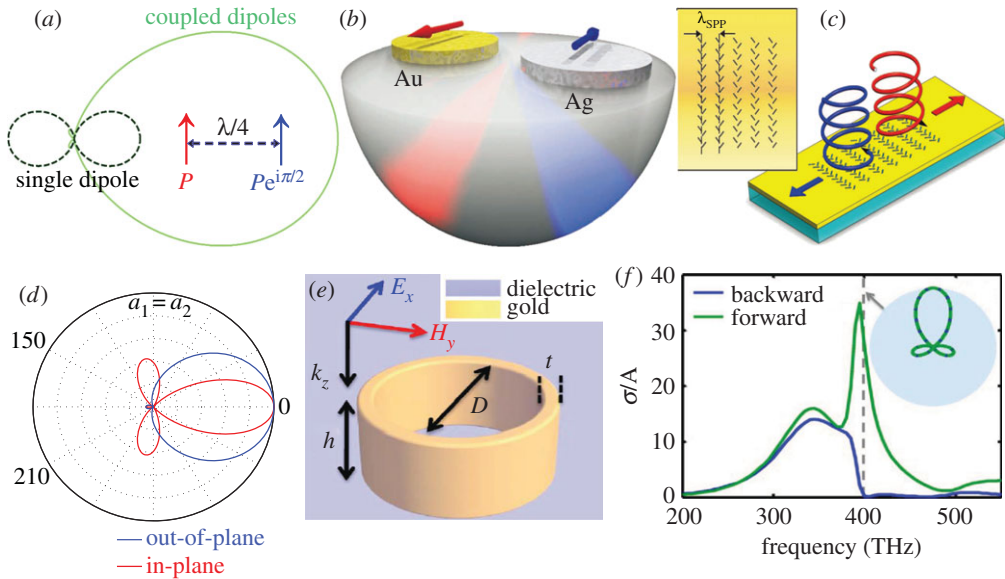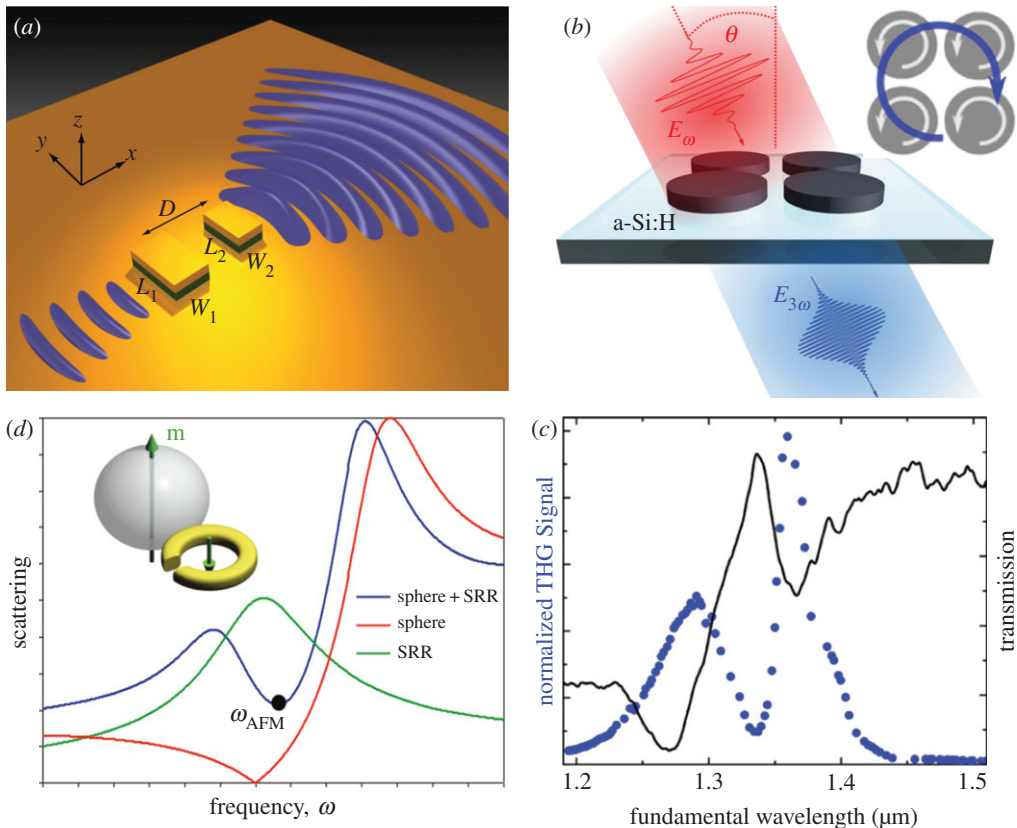
Figure 2. Interferences between electric multipoles. (*a*) In-plane scattering patterns of a single dipole (dashed curve) and two separated dipoles (solid curve). The two dipoles are of the same magnitude and they possess a $\pi/2$ phase difference. The distance between them is $\lambda/4$, where λ is the effective wavelength of the interfering fields. (*b*) The interferences of two EDs supported by metal discs can route light of different colours to different directions. (*c*) A flat metasurface consisting of perpendicular metal-bar pairs as unit cells can couple incident circularly polarized light into SPP waves propagating in opposite directions which are helicity-dependent. To enhance the coupling efficiency, the horizontal periodicity is designed to be the effective wavelength of the SPP waves (λ_{SPP}). (*d*) In-plane (red curve) and out-of-plane (blue curve) scattering patterns of the spherical particle with simultaneous dipole and quadrupole excitation ($a_1 = a_2$). (*f*) Perfect backward scattering elimination and forward scattering enhancement obtained by a metal ring (*e*) through interferences of the electric dipole and quadrupole modes. The inset in (*f*) shows the full in-plane angular scattering pattern. Adapted from: (*a*) [20], (*b*) [21], (*c*) [22], (*d*) [23] and (*e*,*f*) [24].

advanced applications [12]. Additionally, the mechanism of coupled EDs can also be employed to shape radiation patterns of point emitters [28,29] and to guide the designs of various metasurfaces to realize different functionalities [9,13,14].

The principles of interferences between EDs can be extended to higher-order electric multipoles, where the simplest case is the spatially overlapping electric dipole and quadrupole modes. One fundamental platform for such an interference is the Mie scattering of spherical particles with incident plane waves [16]. A parity analysis shows that the electric multipoles of adjacent orders can interfere constructively and destructively in the forward and backward directions, respectively [23]. In figure 2*d*, we show the scattering of the interfering electric dipole and quadrupole (with equal scattering coefficients $a_1 = a_2$), where a highly asymmetric scattering pattern can be obtained [4,23]. Such principle can certainly be applicable to other relatively irregular structures, such as split ring resonators [30] and V-antennas [31,32].

To fully eliminate the scattering at the backward direction (in figure 2*d*, the backward scattering is suppressed but not fully eliminated), the scattering coefficients should satisfy the condition of $3a_1 = 5a_2$, which is challenging to meet as it involves the perfect matching for both real and imaginary parts of the scattering coefficients. This has recently been achieved within a metal ring (figure 2*e*), where the backward scattering can be fully eliminated, while the forward scattering is enhanced (see figure 2*f* and the inset) with properly tuned multipole amplitude and phase [24]. We note that here we confine our discussion to the case of spatially overlapping two multipoles of low orders, and a more exhaustive employment of electric multipolar interferences can involve more spatially separated multipoles of higher orders [4,33], which can provide much more flexibilities for nanoscale light control.

Figure 3. Interferences between magnetic multipoles. (*a*) Two interfering metal–dielectric resonators, which can be viewed as two MDs, can couple the incident light into SPP waves propagating mainly along one preferred direction. (*b*) All-dielectric quadrumer made of a-Si:H discs supports both narrow MDs by each individual disc and a broad collective MD (see inset), which can interfere with one another to produce the magnetic Fano resonance, and (*c*) the corresponding spectra for both fundamental wave and normalized third-harmonic generation. At the Fano dip close to the fundamental wavelength of 1.35 μm, there is significant near-field enhancement within the quadrumer, which leads to significant enhancement for third-harmonic generation. (*d*) Scattering intensity spectra for a single SRR, a single dielectric sphere, and coupled SRR and dielectric sphere. The strong coupling among the individual resonances can render the two MDs out of phase (see inset), leading to the effective antiferromagnetic structures. Adapted from: (*a*) [34], (*b,c*) [35] and (*d*) [36].

3. Magnetic multipoles

The symmetry of Maxwell's equations explains that the electric and magnetic multipoles share some common properties: for example, EDs and MDs oriented along the same direction would have identical radiation patterns [1,15,16]. Generally speaking, all the principles discussed in §2 for the electric multipolar interferences can be directly mapped to the case of magnetic multipoles. For example, the mechanism revealed in figure 2*a* applies equally to the case of two coupled MDs, when highly asymmetric scattering patterns can be also obtained. Nevertheless, the magnetic responses of nanostructures attracted a special attention only recently after the emergence of the field of metamaterials, where the concept of optically induced magnetic response is playing a central role [7,8]. Many types of effective magnetic multipoles have been found to exist not only in traditional plasmonic nanostructures, but also in all-dielectric structures [10,11,13]. This fosters many studies focusing on extending light manipulation principles based on the interferences of electric multipoles to the case of magnetic multipoles and their combinations. As an example, in figure 3*a* we show the interferences of two coupled metal–dielectric resonators which can be viewed as a pair of MDs [34]. Similar to the case shown in figure 2*b*, the two resonators are of

different sizes and thus of different complex polarizabilities, which defines the intrinsic phase difference between them. This polarizability-induced phase, together with the phase accumulated along the gap between two resonators, can render the incident wave coupled to the SPP modes propagating along one preferred direction.

Another notable example of the direct mapping from electric to magnetic multipoles is the magnetic Fano resonances observed for all-dielectric nanoparticle clusters or nanoparticle arrays [35,37–39], being somewhat analogous to the electric Fano resonance observed for metallic particle counterparts [4,38,40]. A recently studied nanodisc quadrumer fabricated of hydrogenated amorphous silicon (a-Si:H) is shown in figure 3b and the spectra for both fundamental wave and normalized third-harmonic generation are shown in figure 3c (incident angle $\theta = \pi/4$) [35]. In brief, an obliquely incident wave can excite simultaneously two kinds of MDs: a narrow MD of each individual dielectric nanodisc and collective broad MD of the whole quadrumer structure [39] (see the inset of figure 3b). The narrow and broad MDs interfere with one another to produce an asymmetric Fano resonance, which is directly driven by optically induced magnetism [4]. This was verified in experiment by measuring the transmission shown in figure 3c. At the Fano dip (close to the fundamental wavelength of 1.35 μm), the fields within the quadrumer can grow significantly, and thus at the Fano resonance the third-harmonic generation can be enhanced dramatically (figure 3c).

Interferences of magnetic multipoles can also produce many other exotic electromagnetic effects, an outstanding example of which is the recently proposed effective optical antiferromagnetism [36]. Figure 3d shows the scattering intensity of antiferromagnetic metamaterials based on compact MD pairs with a π phase difference supported, respectively, by a split-ring resonator (SRR) and dielectric sphere [36]. Basically, the strong coupling between multiple resonances can render the two MDs out of phase even though they are very close to each other (see the inset in figure 3d), leading to an effectively overall staggered (or antiferromagnetic) ordering of the optically induced magnetic moments.

It is worth mentioning that, although in this section we have discussed the interferences of magnetic multipoles, this does not mean that there are no contributions of electric multipoles. Actually in the configuration shown in figure 3d the role played by EDs of the dielectric sphere is crucial, without which the out-of-phase MD pairs and thus the effective antiferromagnetism is not accessible. Moreover, not only the collective MD but also individual MDs shown in figure 3a,b can be interpreted alternatively as a combination of out-of-phase EDs. A notable simple example of this is that within strongly coupled metal bars (which if isolated can be interpreted as an ED), MDs can be effectively excited [41,42]. For the configurations shown in figure 1b,c, as the metallic nanoparticles are well separated and thus not strongly coupled to each other, the mechanism of two-ED interference shown figure 1a is still applicable. In principle, however, all photonic non-magnetic structures can be decomposed into many interacting discrete small EDs [43], and the electromagnetic effects can be explained by the interferences of those EDs only. Nevertheless, under most circumstances the adoption of the concept of magnetic multipoles and higher-order electric multipoles can render deeper physical insights and bring great convenience for various structure designs and applications. We note that here we restrict our discussions to MDs only. Similar to the electric multipoles discussed in §2, such consideration can be naturally extended to higher-order magnetic multipoles, the excitation of which is highly accessible for various structures, especially those high permittivity dielectric particles (see [11,13,14] and references therein). It is actually easy to obtain the magnetic counterparts of what is shown in figure 2d,e and many other electric multipolar interference effects.

4. Electric and magnetic multipoles

In nanophotonics, the incorporation of magnetic responses provides an extra degree of freedom for efficient light control through interfering electric and magnetic multipoles [10,11,13,14]. One of the most notable examples is the recent demonstration of simultaneous forward scattering enhancement and backward scattering suppression based on interferences of EDs and MDs
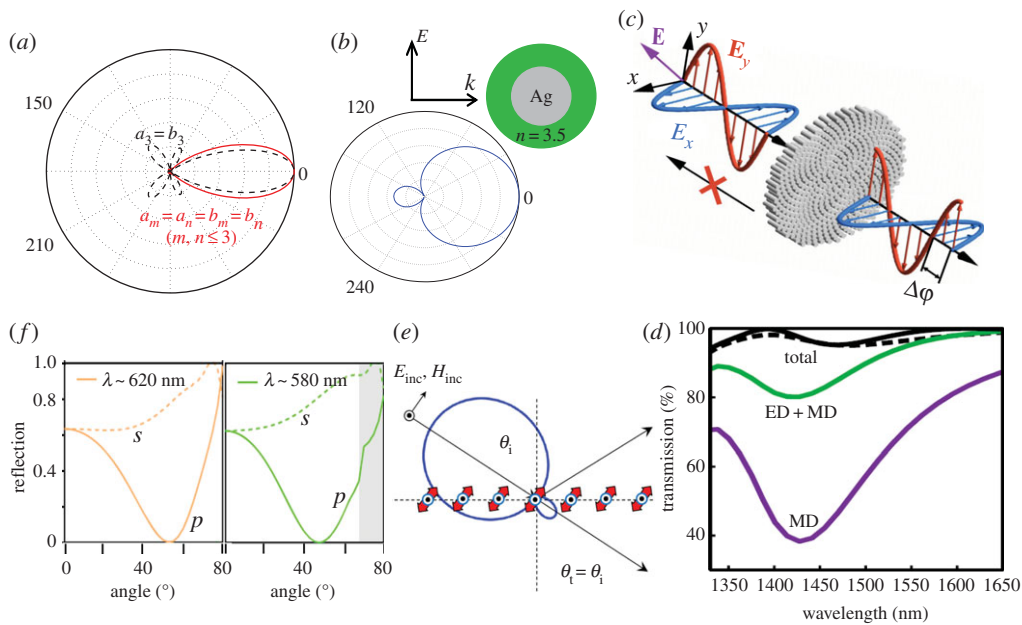
Figure 4. Interferences between electric and magnetic multipoles. (*a*) Mie scattering patterns of spherical particles by incident plane waves. Dashed curve: overlapping electric and magnetic octopoles only with the same magnitude ($a_3 = b_3$); solid curve: overlapping electric and magnetic dipoles, quadrupoles and octopoles with the same corresponding scattering coefficients ($a_m = a_n = b_m = b_n$ (m, $n \leq 3$)). (*b*) Mie scattering pattern of a core–shell nanowire by an incident TM plane wave. The nanorods support overlapping ED and MD, and the magnitude of ED is twice of that of MD, leading to scattering elimination at $\theta = 2/3\pi$ and $4/3\pi$. (*c*) Silicon nanorod metasurface with suppressed reflection and flexible transmission phase control, and (*d*) the transmission spectra (with also the contribution from MD, and the joint contribution of ED and MD). (*e*) An array of meta-atoms made of perpendicular ED–MD dipole-pairs of which the scattering suppression angle can be controlled. (*f*) The wavelength-dependent reflection–incident angle spectra (for both *p* (solid) and *s* (dashed) polarized reflected waves) of the metasurface consisting of a two-dimensional square lattice of silicon spheres. The incident wave is *p*-polarized. Adapted from: (*a*) [23], (*b*) [47], (*c*,*d*) [48] and (*e*,*f*) [49].

(the so-called Kerker scattering) [11,44]. The simplest case of dipolar Kerker scattering and its applications in various nanostructures including metasurfaces have been discussed extensively in several reviews [10,11,13,14], and recently such principle has been applied for strongly coupled particle clusters [45] and antennas made of switchable phase-change materials [46]. Here focus is on two generalizations of the dipolar Kerker scattering: the scattering based on interference of electric and magnetic multipoles of higher orders, and electric and magnetic multipoles of different magnitudes and phases.

For the seminal problem of Mie scattering by spherical particles, it is shown that electric and magnetic multipoles of the same order show opposite parities with respect to $\cos\theta$ (θ is the scattering angle with respect to the forward direction) [23]. This means that simultaneous forward scattering enhancement and backward scattering suppression can be achieved for not only interfering EDs and MDs, but also for any higher order multipoles where the forward scattering directionality can be further enhanced [23]. In figure 4*a*, we show the scattering pattern of interfering electric and magnetic octopoles only (dashed curve, $a_3 = b_3$, other multipoles are negligible). Compared to the dipolar case [23,50], the enhanced forward scattering is more directional, but with several side scattering lobes. To suppress the side scattering lobes, the interferences between the same type of multipoles of different orders (as discussed in §2 and shown in figure 2*d*) can be employed. We further show in figure 4*a* the scattering pattern produced by interfering electric and magnetic dipoles, quadrupoles and octopoles with the same corresponding scattering coefficients (solid curve, $a_m = a_n = b_m = b_n$ (m, $n \leq 3$)). It is clear that

the side scattering has been eliminated without compromising much of the forward scattering directionality. Such an approach to optimize the scattering directionality based on generalized Kerker scattering has been realized for plasmonic core–shell particles, for gap SPP resonators on substrate [51], for coupled dipolar emitter and dielectric–magnetic particle systems [52–54], and for generated nonlinear harmonic waves [55–58].

The Kerker scattering can also be generalized along another direction to electric and magnetic multipoles of different amplitudes and phases, where then the scattering elimination can be achieved for other angles required [47,49]. In figure 4*b*, we show the two-dimensional transverse-magnetic (TM) wave scattering by a metal core–dielectric shell nanowire, where the EDs and MDs can be tuned to spectrally overlap [47]. As the ED corresponds to two degenerate channels, the magnitude of ED is twice of that of the MD, rendering the scattering elimination at scattering angles of $\theta = 2/3\pi$ and $4/3\pi$ rather than the backward direction. Such interference induced control of scattering elimination angle can be also realized in three-dimensional spheres through tuning the EDs and MDs supported [49].

When applied to metasurfaces [9,13,14], the two versions of generalized Kerker scattering discussed above can provide new stimuli and physical insights [48,49,59,60]. In figure 4*c*, we show a metasurface consisting of silicon nanorods, which support not only EDs and MDs, but also higher order multipoles [48]. The total transmission spectra of such a metasurface is shown in figure 4*d*, where the contributions from MD and a combination of ED and MD are also shown. It is clear that the excitation of higher order multipoles besides dipoles contributes to the outstanding feature of broadband near-unity transmission of such a metasurface, the mechanism of which is exactly the generalized Kerker scattering discussed above (figure 4*a*). Moreover, the coexistence of higher order electric and magnetic multipoles also provides much more flexibilities for phase control of the transmitted wave, enabling the functionality of highly efficient polarization control [48].

The other case of generalized Kerker scattering can be employed to metasurfaces based on which the concept of Brewster angle can be broadened [49]. As shown in figure 4*e*, if we arrange the meta-atom consisting of a pair of perpendicular ED and MD (the angle of scattering elimination can be controlled through tuning the dipolar magnitude and phase) into arrays on a surface, the angle of zero scattering from such an array can be tuned. In figure 4*f*, we show the wavelength-dependent reflection–incident angle spectra (for both *p*- and *s*-polarized reflected waves; the incident wave is *p*-polarized with the electric field on the incident plane) for a metasurface made of a two-dimensional square lattice of silicon spheres. For each sphere at different wavelengths, the ratios between the magnitudes of EDs and MDs vary, leading to scattering suppression at different angles [47,49]. For a square lattice of such spheres, this would result in the wavelength-dependent Brewster angles, as verified in figure 4*f*. Moreover, the wavelength-dependent Brewster angle can be also observed for *s*-polarized incident waves [49], which is unaccessible at conventional interfaces where there is only dominant ED excitation. Here, we discuss only the scattering suppression at different angles based on interferences between ED and MD, which can certainly be extended to higher order multipoles.

5. Electric and toroidal multipoles

Though dynamic toroidal multipoles play an essential role in the expansions for arbitrary charge–current distributions [15,17], they had not attracted much attention until the recent demonstration of TDs in engineered metamaterials [19]. This is largely due to the fact that in the far field toroidal multipoles are identical to their electric multipolar counterparts [17]. At the same time, conventional multipole expansions are usually conducted for charge–current distributions that are far smaller than the effective wavelength, where the contributions of toroidal multipoles are negligible [15,18]. Though the isolated excitation of dynamic toroidal multipoles would require careful structure engineering to match the special corresponding near-field current distributions [17,19], it is also shown recently that even simple homogeneous dielectric particles can support TDs [18,61–63], though they are co-excited with the electric and magnetic multipoles.
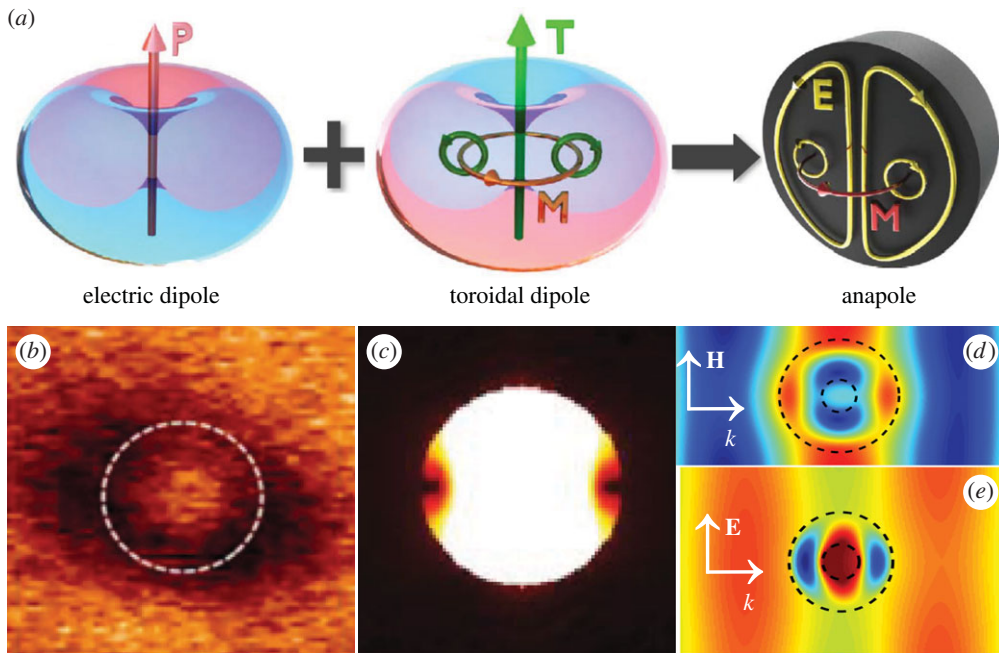
Figure 5. Interferences between electric and toroidal multipoles. (*a*) The destructive interference of an ED (left) and a TD (middle) leads to the formation of a non-radiating anapole mode. The near-field distributions for the anapole modes excited within: (*b*) silicon nanodisc with plane wave incidence; (*c*) all-dielectric nanosphere with two counter propagating radially polarized beams of the same intensity but out of phase (the incident wave is subtracted from the field distribution plot); (*d*,*e*) metal–dielectric core–shell nanowires of both polarized incident plane waves. Adapted from: (*a*,*b*) [61], (*c*) [64] and (*d*,*e*) [63]. (Online version in colour.)

Roughly speaking, to effectively support dynamic TDs, the excitation of out-of-phase MDs is required. Even for the fundamental homogeneous spherical and cylindrical structures, such out-of-phase MDs can be excited for relatively large particle sizes, leading to the effective formation of dynamic TDs [18,61–63]. The excitation of TDs within composite structures has been discussed in detail in [17], and here we focus on the excitation of TDs within individual nanoparticles and their interferences with the electric counterparts (EDs).

Since the EDs and TDs have identical scattering patterns, it means that when co-excited and spatially overlapped with the same scattering magnitude but out of phase, they can cancel the scattering of each other in the far field, appearing to be invisible [17,61] (figure 5*a*). This is the basic mechanism of the recently discovered non-radiating anapoles [61]. To observe a pure non-radiating anapole excitation, besides proper ED and TD excitation, the suppression of other multipoles is also required. This is not possible for homogeneous spheres or cylinders with incident plane waves as the MDs and other quardupolar excitations at the ED–TD scattering cancelling point are non-eligible [18,61–63]. The anapole excitation has been firstly experimentally realized within engineered composite metallic metamaterials in the microwave regime, where the excitation of other multipoles is negligible [65]. The pure anapole excitation can be also achieved with other unwanted multipoles suppressed within the following individual nanoparticles in the optical regime: (i) all-dielectric nanodiscs with incident plane waves [61] (as is shown in figure 5*b* of the experimental near-field enhancement close to the silicon nanodisc at the anapole point); (ii) all-dielectric spheres with engineered incident waves (two counter propagating radially polarized beams with the same intensity but out of phase) [64]; the electric field distribution (incident wave subtracted) is shown in figure 5*c* at the anapole point; and (iii) core–shell metal–dielectric nanospheres or nanorods with incident plane waves [62,63]. Figure 5*d*,*e* shows the electric field distributions of the core–shell cylinders for both polarizations of the incident plane

waves at the anapole point [63]. For both cases the incident wave has experienced almost no perturbations, verifying the non-radiative nature of the anapole mode excited. It is recently also shown that for homogeneous spherical particles with incident plane waves, the radial anisotropy can be employed for pure anapole excitation [66]. The efficient excitation of non-radiating anapoles can play a significant role for improving nonlinear conversion efficiency and enhancing absorption in photonic nanostructures [67,68]. It is worth mentioning that here we confine our discussions to anapoles induced by interferences between ED and TD only, and it is natural to extend the discussions to higher order anapoles, which are induced by the scattering cancellation of a pair of electric and toroidal multipoles of higher orders [17].

6. Concluding remarks and outlook

As a source of electromagnetic fields, excited electric charges and currents can generate multipole modes of different types and orders, and their interferences decide many important electromagnetic effects at the nanoscale. Here, we have discussed the multipolar interference effects in resonant metallic, metal–dielectric and dielectric nanophotonics structures. More specifically, we have presented a coherent view into interference effects involving electric, magnetic and toroidal multipoles, and have shown that such interferences lead directly to many exotic nanophotonic effects, such as ultra-directional propagation of light, optical antiferromagnetism, generalized Kerker scattering and Brewster angle, as well as recently discovered non-radiating optical anapoles. A complete employment of interferences between all sorts of multipoles of different types and orders relying on both amplitude and phase engineering can provide much more flexibilities for nanoscale manipulation of free-space light propagation and light–matter interaction, which might incubate and stimulate new ideas for fundamental researches and many applications in nanophotonics.

As marked by the red double arrow and circle in figure 1*a*, the interferences between toroidal multipoles and those between magnetic and toroidal multipoles have not been well studied in the existing literature. Nevertheless, as electric and toroidal multipoles of the same order have identical scattering patterns, it is natural to expect that the basic principles discussed in §2 for electric multipoles can be mapped directly to toroidal multipoles, meaning that interferences of toroidal multipoles can also be employed to produce highly directional light propagation and to realize the toroidal Fano resonances. The mechanisms discussed in §4 for interferences between electric and magnetic multipoles can also be applied directly to magnetic and toroidal multipoles, indicating that the generalized Kerker scattering and Brewster angle are also accessible based on interferences between magnetic and toroidal multipoles. We note that even for the well-studied cases discussed in §§2–5, most studies are confined to interferences of low-order multipoles (up to quadrupoles only). Moreover, the multipolar interference can also result in other exotic phenomena, including chiral and birefringent effects in nanophotonics [7,69–71], and actually the optical chirality can involve the interacting multipoles from all three families [17,71]. Basically, there are still many intriguing topics to explore in this research field, and a thorough investigation and exploitation of interferences between multipoles of higher orders and of all three major families would give more impetus to the progress of nanophotonics. Additionally, the analysis based on multipole expansions and interferences can also be extended to newly emerging fields that hybridize quickly with the subject of nanophotonics, such as quantum photonics [72,73], two-dimensional flatland photonics [74] and topological photonics [75]. The analysis of multipolar interference effects in those interdisciplinary fields may help to gain deeper physical insights into many electromagnetic effects, which might foster more fundamental research and stimulate advanced applications.

References

1. Novotny L, Hecht B. 2012 *Principles of nano-optics*. Cambridge, UK: Cambridge University Press.
2. Kabashin AV, Evans P, Pastkovsky S, Hendren W, Wurtz GA, Atkinson R, Pollard R, Podolskiy VA, Zayats AV. 2009 Plasmonic nanorod metamaterials for biosensing. *Nat. Mater.* **8**, 867–871. (doi:10.1038/nmat2546)
3. Atwater HA, Polman A. 2010 Plasmonics for improved photovoltaic devices. *Nat. Mater.* **9**, 205–213. (doi:10.1038/nmat2629)
4. Luk'yanchuk B, Zheludev NI, Maier SA, Halas NJ, Nordlander P, Giessen H, Chong CT. 2010 The Fano resonance in plasmonic nanostructures and metamaterials. *Nat. Mater.* **9**, 707–715. (doi:10.1038/nmat2810)
5. Miroshnichenko AE, Flach S, Kivshar YS. 2010 Fano resonances in nanoscale structures. *Rev. Mod. Phys.* **82**, 2257–2298. (doi:10.1103/RevModPhys.82.2257)
6. Novotny L, Van Hulst N. 2011 Antennas for light. *Nat. Photonics* **5**, 83–90. (doi:10.1038/nphoton.2010.237)
7. Soukoulis CM, Wegener M. 2011 Past achievements and future challenges in the development of three-dimensional photonic metamaterials. *Nat. Photonics* **5**, 523–530. (doi:10.1038/nphoton.2011.154)
8. Zheludev NI, Kivshar YS. 2012 From metamaterials to metadevices. *Nat. Mater.* **11**, 917–924. (doi:10.1038/nmat3431)
9. Kildishev AV, Boltasseva A, Shalaev VM. 2013 Planar photonics with metasurfaces. *Science* **339**, 1232009. (doi:10.1126/science.1232009)
10. Krasnok AE, Maksymov IS, Denisyuk AI, Belov PA, Miroshnichenko AE, Simovski CR, Kivshar YS. 2013 Optical nanoantennas. *Phys.-Uspekhi* **56**, 539–564. (doi:10.3367/UFNe.0183.201306a.0561)
11. Liu W, Kivshar YS, Miroshnichenko AE. 2014 Control of light scattering by nanoparticles with optically-induced magnetic responses. *Chin. Phys. B* **23**, 047806. (doi:10.1088/1674-1056/23/4/047806)
12. Bliokh KY, Rodríguez-Fortuño FJ, Nori F, Zayats AV. 2015 Spin-orbit interactions of light. *Nat. Photonics* **9**, 796–808. (doi:10.1038/nphoton.2015.201)
13. Kuznetsov AI, Miroshnichenko AE, Brongersma ML, Kivshar YS, Luk'yanchuk B. 2016 Optically resonant dielectric nanostructures. *Science* **354**, 838–846. (doi:10.1126/science.aag2472)
14. Chen HT, Taylor AJ, Yu N. 2016 A review of metasurfaces: physics and applications. *Rep. Prog. Phys.* **79**, 076401. (doi:10.1088/0034-4885/79/7/076401)
15. Jackson JD, Jackson JD. 1962 *Classical electrodynamics*, vol. 3. New York, NY: Wiley.
16. Bohren CF, Huffman DR. 2008 *Absorption and scattering of light by small particles*. New York, NY: John Wiley & Sons.
17. Papasimakis N, Fedotov VA, Savinov V, Raybould TA, Zheludev NI. 2016 Electromagnetic toroidal excitations in matter and free space. *Nat. Mater.* **15**, 263–271. (doi:10.1038/nmat4563)
18. Liu W, Shi J, Lei B, Hu H, Miroshnichenko AE. 2015 Efficient excitation and tuning of toroidal dipoles within individual homogenous nanoparticles. *Opt. Express* **23**, 24738–24747. (doi:10.1364/OE.23.024738)
19. Kaelberer T, Fedotov VA, Papasimakis N, Tsai DP, Zheludev NI. 2010 Toroidal dipolar response in a metamaterial. *Science* **330**, 1510–1512. (doi:10.1126/science.1197172)
20. Miroshnichenko AE, Kivshar YS. 2013 Polarization traffic control for surface plasmons. *Science* **340**, 283–284. (doi:10.1126/science.1236154)
21. Shegai T, Chen S, Miljković VD, Zengin G, Johansson P, Käll M. 2011 A bimetallic nanoantenna for directional colour routing. *Nat. Commun.* **2**, 481. (doi:10.1038/ncomms1490)
22. Lin J, Mueller JPB, Wang Q, Yuan G, Antoniou N, Yuan XC, Capasso F. 2013 Polarization-controlled tunable directional coupling of surface plasmon polaritons. *Science* **340**, 331–334. (doi:10.1126/science.1233746)

23. Liu W, Zhang J, Lei B, Ma H, Xie W, Hu H. 2014 Ultra-directional forward scattering by individual core-shell nanoparticles. *Opt. Express* **22**, 16 178–16 187. (doi:10.1364/OE.22.016178)
24. Alaee R, Filter R, Lehr D, Lederer F, Rockstuhl C. 2015 A generalized Kerker condition for highly directive nanoantennas. *Opt. Lett.* **40**, 2645–2648. (doi:10.1364/OL.40.002645)
25. Wilczek F, Shapere A. 1989 *Geometric phases in physics*, vol. 5. Singapore: World Scientific.
26. Bomzon Z, Kleiner V, Hasman E. 2001 Pancharatnam–Berry phase in space-variant polarization-state manipulations with subwavelength gratings. *Opt. Lett.* **26**, 1424–1426. (doi:10.1364/OL.26.001424)
27. Huang L, Chen X, Bai B, Tan Q, Jin G, Zentgraf T, Zhang S. 2013 Helicity dependent directional surface plasmon polariton excitation using a metasurface with interfacial phase discontinuity. *Light Sci. Appl.* **2**, e70. (doi:10.1038/lsa.2013.26)
28. Bonod N, Devilez A, Rolly B, Bidault S, Stout B. 2010 Ultracompact and unidirectional metallic antennas. *Phys. Rev. B* **82**, 115429. (doi:10.1103/PhysRevB.82.115429)
29. Rolly B, Stout B, Bidault S, Bonod N. 2011 Crucial role of the emitter–particle distance on the directivity of optical antennas. *Opt. Lett.* **36**, 3368–3370. (doi:10.1364/OL.36.003368)
30. Hancu IM, Curto AG, Castro-López M, Kuttge M, van Hulst NF. 2014 Multipolar interference for directed light emission. *Nano Lett.* **14**, 166–171. (doi:10.1021/nl403681g)
31. Vercruysse D *et al.* 2014 Directional fluorescence emission by individual V-antennas explained by mode expansion. *ACS Nano* **8**, 8232–8241. (doi:10.1021/nn502616k)
32. Li J, Verellen N, Vercruysse D, Bearda T, Lagae L, Van Dorpe P. 2016 All-dielectric antenna wavelength router with bidirectional scattering of visible light. *Nano Lett.* **16**, 4396–4403. (doi:10.1021/acs.nanolett.6b01519)
33. Zhang S, Genov DA, Wang Y, Liu M, Zhang X. 2008 Plasmon-induced transparency in metamaterials. *Phys. Rev. Lett.* **101**, 047401. (doi:10.1103/PhysRevLett.101.047401)
34. Liu Y, Palomba S, Park Y, Zentgraf T, Yin X, Zhang X. 2012 Compact magnetic antennas for directional excitation of surface plasmons. *Nano Lett.* **12**, 4853–4858. (doi:10.1021/nl302339z)
35. Shorokhov AS *et al.* 2016 Multifold enhancement of third-harmonic generation in dielectric nanoparticles driven by magnetic Fano resonances. *Nano Lett.* **16**, 4857–4861. (doi:10.1021/acs.nanolett.6b01249)
36. Miroshnichenko AE, Luk'yanchuk B, Maier SA, Kivshar YS. 2012 Optically induced interaction of magnetic moments in hybrid metamaterials. *ACS Nano* **6**, 837–842. (doi:10.1021/nn204348j)
37. Evlyukhin AB, Reinhardt C, Seidel A, Luk'yanchuk BS, Chichkov BN. 2010 Optical response features of Si-nanoparticle arrays. *Phys. Rev. B* **82**, 045404. (doi:10.1103/PhysRevB.82.045404)
38. Miroshnichenko AE, Kivshar YS. 2012 Fano resonances in all-dielectric oligomers. *Nano Lett.* **12**, 6459–6463. (doi:10.1021/nl303927q)
39. Hopkins B, Filonov DS, Miroshnichenko AE, Monticone F, Alù A, Kivshar YS. 2015 Interplay of magnetic responses in all-dielectric oligomers to realize magnetic Fano resonances. *ACS Photonics* **2**, 724–729. (doi:10.1021/acsphotonics.5b00082)
40. Liu W, Miroshnichenko AE, Neshev DN, Kivshar YS. 2012 Polarization-independent Fano resonances in arrays of core-shell nanoparticles. *Phys. Rev. B* **86**, 081407. (doi:10.1103/PhysRevB.86.081407)
41. Svirko Y, Zheludev N, Osipov M. 2001 Layered chiral metallic microstructures with inductive coupling. *Appl. Phys. Lett.* **78**, 498–500. (doi:10.1063/1.1342210)
42. Shalaev VM, Cai W, Chettiar UK, Yuan HK, Sarychev AK, Drachev VP, Kildishev AV. 2005 Negative index of refraction in optical metamaterials. *Opt. Lett.* **30**, 3356–3358. (doi:10.1364/OL.30.003356)
43. Draine BT, Flatau PJ. 1994 Discrete-dipole approximation for scattering calculations. *J. Opt. Soc. Am. A* **11**, 1491–1499. (doi:10.1364/JOSAA.11.001491)
44. Kerker M, Wang DS, Giles CL. 1983 Electromagnetic scattering by magnetic spheres. *J. Opt. Soc. Am.* **73**, 765–767. (doi:10.1364/JOSA.73.000765)
45. Yao K, Liu Y. 2016 Controlling electric and magnetic resonances for ultracompact nanoantennas with tunable directionality. *ACS Photonics* **3**, 953–963. (doi:10.1021/acsphotonics.5b00697)
46. Alaee R, Albooyeh M, Tretyakov S, Rockstuhl C. 2016 Phase-change material-based nanoantennas with tunable radiation patterns. *Opt. Lett.* **41**, 4099–4102. (doi:10.1364/OL.41.004099)

47. Liu W, Miroshnichenko AE, Oulton RF, Neshev DN, Hess O, Kivshar YS. 2013 Scattering of core-shell nanowires with the interference of electric and magnetic resonances. *Opt. Lett.* **38**, 2621–2624. (doi:10.1364/OL.38.002621)

48. Kruk S, Hopkins B, Kravchenko II, Miroshnichenko A, Neshev DN, Kivshar YS. 2016 Broadband highly efficient dielectric metadevices for polarization control. *APL Photonics* **1**, 030801. (doi:10.1063/1.4949007)

49. Paniagua-Domínguez R *et al.* 2016 Generalized Brewster effect in dielectric metasurfaces. *Nat. Commun.* **7**, 10362. (doi:10.1038/ncomms10362)

50. Liu W, Miroshnichenko AE, Neshev DN, Kivshar YS. 2012 Broadband unidirectional scattering by magneto-electric core-shell nanoparticles. *ACS Nano* **6**, 5489–5497. (doi:10.1021/nn301398a)

51. Pors A, Andersen SK, Bozhevolnyi SI. 2015 Unidirectional scattering by nanoparticles near substrates: generalized Kerker conditions. *Opt. Express* **23**, 28 808–28 828. (doi:10.1364/OE.23.028808)

52. Rolly B, Geffrin JM, Abdeddaim R, Stout B, Bonod N. 2013 Controllable emission of a dipolar source coupled with a magneto-dielectric resonant subwavelength scatterer. *Sci. Rep.* **3**, 3063. (doi:10.1038/srep03063)

53. Krasnok AE, Simovski CR, Belov PA, Kivshar YS. 2014 Superdirective dielectric nanoantennas. *Nanoscale* **6**, 7354–7361. (doi:10.1039/c4nr01231c)

54. Rusak E, Staude I, Decker M, Sautter J, Miroshnichenko AE, Powell DA, Neshev DN, Kivshar YS. 2014 Hybrid nanoantennas for directional emission enhancement. *Appl. Phys. Lett.* **105**, 221109. (doi:10.1063/1.4903219)

55. Smirnova DA, Kivshar YS. 2016 Multipolar nonlinear nanophotonics. (https://arxiv.org/abs/1609.02057)

56. Wang L *et al.* 2016 Multipolar third-harmonic generation in fishnet metamaterials. *ACS Photonics* **3**, 1494–1499. (doi:10.1021/acsphotonics.6b00040)

57. Carletti L, Locatelli A, Neshev D, De Angelis C. 2016 Shaping the radiation pattern of second-harmonic generation from AlGaAs dielectric nanoantennas. *ACS Photonics* **3**, 1500–1507. (doi:10.1021/acsphotonics.6b00050)

58. Smirnova DA, Khanikaev AB, Smirnov LA, Kivshar YS. 2016 Multipolar third-harmonic generation driven by optically induced magnetic resonances. *ACS Photonics* **3**, 1468–1476. (doi:10.1021/acsphotonics.6b00036)

59. Yang Y, Wang W, Moitra P, Kravchenko II, Briggs DP, Valentine J. 2014 Dielectric meta-reflectarray for broadband linear polarization conversion and optical vortex generation. *Nano Lett.* **14**, 1394–1399. (doi:10.1021/nl4044482)

60. Proust J, Bedu F, Gallas B, Ozerov I, Bonod N. 2016 All-dielectric colored metasurfaces with silicon Mie resonators. *ACS Nano* **10**, 7761–7767. (doi:10.1021/acsnano.6b03207)

61. Miroshnichenko AE, Evlyukhin AB, Yu YF, Bakker RM, Chipouline A, Kuznetsov AI, Luk'yanchuk B, Chichkov BN, Kivshar YS. 2015 Nonradiating anapole modes in dielectric nanoparticles. *Nat. Commun.* **6**, 8069. (doi:10.1038/ncomms9069)

62. Liu W, Zhang J, Miroshnichenko AE. 2015 Toroidal dipole-induced transparency in core-shell nanoparticles. *Laser Photonics Rev.* **9**, 564–570. (doi:10.1002/lpor.201500102)

63. Liu W, Zhang J, Lei B, Hu H, Miroshnichenko AE. 2015 Invisible nanowires with interfering electric and toroidal dipoles. *Opt. Lett.* **40**, 2293–2296. (doi:10.1364/OL.40.002293)

64. Wei L, Xi Z, Bhattacharya N, Urbach HP. 2016 Excitation of the radiationless anapole mode. *Optica* **3**, 799. (doi:10.1364/OPTICA.3.000799)

65. Fedotov VA, Rogacheva AV, Savinov V, Tsai DP, Zheludev NI. 2013 Resonant transparency and non-trivial non-radiating excitations in toroidal metamaterials. *Sci. Rep.* **3**, 02967. (doi:10.1038/srep02967)

66. Liu W, Lei B, Shi J, Hu H, Miroshnichenko AE. 2015 Elusive pure anapole excitation in homogenous spherical nanoparticles with radial anisotropy. *J. Nanomater.* **2015**, 672957. (doi:10.1155/2015/672957)

67. Grinblat G, Li Y, Nielsen MP, Oulton RF, Maier SA. 2016 Enhanced third harmonic generation in single germanium nanodisks excited at the anapole mode. *Nano Lett.* **16**, 4635–4640. (doi:10.1021/acs.nanolett.6b01958)

68. Wang R, Dal Negro L. 2016 Engineering non-radiative anapole modes for broadband absorption enhancement of light. *Opt. Express* **24**, 19048. (doi:10.1364/OE.24.019048)

69. Zhang S, Park YS, Li J, Lu X, Zhang W, Zhang X. 2009 Negative refractive index in chiral metamaterials. *Phys. Rev. Lett.* **102**, 023901. (doi:10.1103/PhysRevLett.102.023901)
70. Plum E, Liu XX, Fedotov VA, Chen Y, Tsai DP, Zheludev NI. 2009 Metamaterials: optical activity without chirality. *Phys. Rev. Lett.* **102**, 113902. (doi:10.1103/PhysRevLett.102.113902)
71. Papasimakis N, Fedotov VA, Marinov K, Zheludev NI. 2009 Gyrotropy of a metamolecule: wire on a torus. *Phys. Rev. Lett.* **103**, 093901. (doi:10.1103/PhysRevLett.103.093901)
72. Tame MS, McEnery KR, Özdemir ŞK, Lee J, Maier SA, Kim MS. 2013 Quantum plasmonics. *Nat. Phys.* **9**, 329–340. (doi:10.1038/nphys2615)
73. Schröder T, Mouradian S, Zheng J, Trusheim ME, Walsh M, Chen EH, Li L, Bayn I, Englund D. 2016 Quantum nanophotonics in diamond. (http://arxiv.org/abs/1603.05339)
74. Xia F, Wang H, Xiao D, Dubey M, Ramasubramaniam A. 2014 Two-dimensional material nanophotonics. *Nat. Photonics* **8**, 899–907. (doi:10.1038/nphoton.2014.271)
75. Lu L, Joannopoulos JD. 2014 Topological photonics. *Nat. Photonics* **8**, 821–829. (doi:10.1038/nphoton.2014.248)

14

rsta.royalsocietypublishing.org *Phil. Trans. R. Soc. A* **375**: 20160317